

tional evidence that the upper lunar crust may be compositionally zoned. The presence of olivine in the Copernicus region suggests a possible magnesium-rich zone of unknown origin in the upper lunar crust. Possible sources of the olivine include (i) a primary cumulate zone resulting from early lunar differentiation, (ii) a singular magma chamber or cumulate zone associated with lunar volcanism and emplaced within the crust in this area, and (iii) a zone of material from either of the above, relocated by an earlier event. A detailed reconstruction of the stratigraphic sequence at this site in light of our current understanding of crater formation dynamics will be essential to put this new compositional information in context with the evolution of the lunar crust.

CARLE M. PIETERS

Department of Geological Sciences,  
Brown University,  
Providence, Rhode Island 02912

#### References and Notes

1. F. El-Baz, "Geologic characteristics of the nine lunar landing mission sites recommended by the group for lunar exploration planning," *Bellcomm TR-68-340-1*; NASA STAR N68-28576 (1968), pp. 32-39; *Eos* 50, 638 (1969).
2. E. M. Shoemaker and R. J. Hackman, *The Moon, Int. Astron. Union Symp.* 14 (1962), p. 289; D. E. Wilhelms and J. McCauley, *U.S. Geol. Surv. Map I-703* (1971).
3. Lunar Orbiter II images 162H3 and V 150, 151, 152, 153, 155, 156, and 157.
4. H. H. Schmitt, N. J. Trask, E. M. Shoemaker, *U.S. Geol. Surv. Map I-515* (1967); K. A. Howard, *U.S. Geol. Surv. Map I-840* (1975).
5. G. W. Ullrich, P. J. Roddy, G. Simmons, in *Impact and Explosion Cratering*, P. J. Roddy *et al.*, Eds. (Pergamon, New York, 1977), p. 959; M. R. Dence, R. A. F. Grieve, B. P. Robertson, in *ibid.*, p. 247; R. J. Pike, in *ibid.*, p. 489.
6. J. W. Head, C. M. Pieters, T. B. McCord, J. B. Adams, S. H. Zisk, *Icarus* 33, 145 (1978).
7. T. B. McCord, M. P. Charette, T. V. Johnson, L. A. Lebofsky, C. Pieters, *Moon* 5, 52 (1972).
8. C. M. Pieters and T. B. McCord, *Proc. 7th Lunar Sci. Conf.* (1976), p. 2677; T. B. McCord, C. M. Pieters, M. A. Feierberg, *Icarus* 29, 1 (1976); T. V. Johnson, J. A. Mosher, D. L. Matson, *Proc. 8th Lunar Sci. Conf.* (1977), p. 1013.
9. C. M. Pieters, *Proc. 9th Lunar Planet. Sci. Conf.* (1978), p. 2825. In this remote sensing study it was shown that two-thirds of lunar basalt types are not represented in the sample collections.
10. T. B. McCord, R. N. Clark, B. R. Hawke, L. A. McFadden, P. D. Owensby, C. M. Pieters, J. B. Adams, *J. Geophys. Res.*, in press.
11. J. B. Adams, in *Infrared and Raman Spectroscopy of Lunar and Terrestrial Materials*, C. Karr, Ed. (Academic Press, New York, 1975), p. 91.
12. ———, *J. Geophys. Res.* 79, 4829 (1974).
13. R. B. Singer, *ibid.*, in press.
14. C. M. Pieters, S. Flamm, T. B. McCord, *Lunar Planet. Sci.* 11, 879 (1980).
15. J. B. Adams, F. Hörz, R. V. Gibbons, *ibid.* 10, 1 (1979).
16. M. J. Gaffey, *J. Geophys. Res.* 81, 905 (1976).
17. This report is dedicated to Tom McGetchin, whose enthusiasm for planetary exploration helped polish many stones. The author is indebted to P. Owensby for her initiative in repeating the key observations of Copernicus. Discussions with J. Head, W. Hale, J. Adams, and T. McCord have helped formulate important aspects of this discussion. C.M.P. was a visiting astronomer at Mauna Kea Observatory, University of Hawaii, and is supported by NASA grants NAGW-28 and NAGW-37.

21 May 1981; revised 21 August 1981

## High-Resolution X-ray Observations of the Orion Nebula

**Abstract.** *Observations of the Trapezium region in the Orion Nebula obtained with the high-resolution x-ray imaging instrument on board the Einstein Observatory reveal at least 58 sources of x-ray emission. All but two of the sources can be identified with visible stars. The strongest x-ray source is the star  $\theta^1C$ , which excites the emission nebula. Its x-ray luminosity is  $6 \times 10^{32}$  ergs per second. The rest of the x-ray sources may be identified with stars of all spectral types. Strong x-ray emission is not observed from members of the infrared cluster embedded within the Orion molecular cloud.*

The Orion Nebula (M42) is the best known and best studied site of recent star formation in our galaxy. Located about 500 pc away and easily identified with a pair of binoculars in the sword of Orion the hunter, the nebulosity is excited by the star  $\theta^1C$ , a member of the Trapezium cluster. An optically opaque cloud of gas and dust is situated behind the nebulosity. Such molecular clouds in our galaxy are believed to be sites of ongoing star formation. Indeed, studies of this cloud by infrared and radio techniques have identified several sites of current star formation within it (1).

We present a deep x-ray image (22,021 seconds of integration) of the Orion Nebula region that was obtained by the high-resolution imaging (HRI) instrument on board the Einstein Observatory (2). This observation was motivated by four considerations. First, the x-ray source in Orion that was discovered by Uhuru was known, from observations by SAS-3 and by the Einstein Observatory arc minute resolution imaging proportional counter (IPC), to be centered on the Trapezium cluster of stars (3-5). The HRI observation thus offered the possibility of identifying and studying the Trapezium source in detail. Second, the serendipitous discovery of x-ray emission from the Cygnus OB2 association demonstrated that hot young stars can be x-ray sources (6). Observation of the Orion association of O and B stars was thus of interest. Third, a deep HRI integration offered the possibility of searching for x-ray emission from the Orion infrared cluster (7). The objects that comprise the cluster are believed to be hot young stars that are forming, or formed very recently, within the molecular cloud. Molecular clouds can be surprisingly transparent to hard x-rays; using the x-ray opacities determined by Cruddace *et al.* (8), we calculate that for a source obscured by 35 magnitudes of visual extinction, at least 10 percent of a 2-keV photon flux penetrates the cloud. Our HRI observation was thus intended, in part, to search for x-ray sources within the cloud and to assess their role in the heating, kinematics, and support of the cloud. Finally, the

IPC observation of a  $1^\circ$  by  $1^\circ$  field centered on the Trapezium cluster revealed 22 sources tentatively identified with stars of early spectral type and stars of the nebular variable class (5). The high angular resolution capability of the HRI offered the means to secure their identifications.

The field of view of the HRI ( $\sim 25$  arc minutes in diameter) was centered near the Trapezium cluster for our observation. The angular resolution is  $\sim 2$  arc seconds (half width at half maximum of the core of the image of a pointlike source) over a circular region of radius  $\sim 5$  arc minutes around the telescope pointing center. The instrument is sensitive to photons with energies of 0.1 to 4 keV; no spectral resolution within this energy range is possible. We obtained 10,720 seconds of data on 2 September 1979, and the remaining 11,301 seconds on 27 September 1979. All the data were added to form a single deep image. Once individual sources were identified in the composite image, the data were repartitioned to investigate the variability of the strongest sources.

The existence and location of the sources were established in two ways. Most of the sources were derived by a computer algorithm developed at the Harvard-Smithsonian Center for Astrophysics; the algorithm calculates the average background level in the field and the counts in each 12 by 12 arc second detection element, and then compares these to a threshold level equal to four times the fluctuation in the background. Fifty sources satisfied this criterion. This algorithm works best for isolated sources but fails for crowded regions. Because the Trapezium region proved to have several sources in very close proximity, we established their existence by direct inspection of maps of counts per detection element. The x-ray sources were then identified by inspection of an overlay of a contour plot of the x-ray image on suitable optical photographs. We established in this manner that a total of 58 sources of x-ray emission were present in the 25 arc minute field. Of these, 51 sources can be unambiguously

identified with a single star, for another five the x-ray resolution element contains at least two stars so that unique identification is not possible, and two have no cataloged optical counterpart.

The source list is given in Table 1. Source coordinates are in columns 2 and 3 of the table and the stellar identification and spectral classification in columns 5 to 7. The x-ray fluxes in column 4 were calculated with an HRI conversion of 1 count per second =  $2.6 \times 10^{-10}$  erg  $\text{cm}^{-2} \text{sec}^{-1}$ , found by comparing HRI to IPC counts. These values are only a guide to the actual x-ray flux because they depend on the spectrum incident on the detector.

Most of the sources in the central 6 arc minutes of our image are also labeled in Fig. 1. Figure 2 shows in detail the x-ray emission from the Trapezium region. Comparison of Fig. 1 and Table 1 reveals several possible x-ray sources that are not established by the source algorithm but appear in Fig. 1 to be associated with

stars (for example,  $\pi 1924$ ,  $\pi 1838$ , and  $\pi 2032$ ). Because their identification and flux are uncertain, these possible sources are not listed in Table 1.

In this report we describe the sources located in the central 6 arc minutes of the HRI image (9). The strongest x-ray source in the Orion region is  $\theta^1\text{C}$  (Figs. 1 and 2 and Table 1). It completely dominates the x-ray emission of the Trapezium region. Its spectral type is O7 (10). The next strongest source in the image is the star  $\theta^1\text{E}$ , which is also in the Trapezium region. Its spectral type was recently determined as F8Vn (11). Figure 2 shows that  $\theta^1\text{F}$  and  $\theta^1\text{A}$  may also be x-ray sources, but their emission cannot be separated, because of the angular resolution, from that of  $\theta^1\text{C}$  and  $\theta^1\text{E}$ . It is also difficult to distinguish this emission from that of several weak point sources. The only other O-type star in the field of view,  $\theta^2\text{A}$  [O9V (12)], is the fourth strongest x-ray source in the field. Both  $\theta^2\text{C}$  and  $\pi 1956$  [B5V and B8IV-V (13, 14)] are

x-ray sources, while other B-type stars such as  $\theta^1\text{B}$  (B3V),  $\theta^1\text{D}$  (B0.5V), and  $\theta^2\text{B}$  (B1V) (13-15) were not detected ( $< 1$  percent of the intensity of  $\theta^1\text{C}$ ). In addition to the two O-type stars, two B-type stars, and one F-type star, two G- and seven K-type stars were detected. Thus, on the basis of this sample of 14 stars with known spectral classification, there is little evidence that stars of a particular spectral type are predisposed toward x-ray emission.

From their analysis of the IPC observation of this region, Ku and Chanan (5) argued that many of the sources detected in the Orion region were stellar and associated with the class of stars identified as nebular variables or pre-main sequence stars (16). Indeed, the third brightest source in the image is MT Ori. In addition, Feigelson and De Campli (17) found that two variable T-Tauri stars in the Orion region are x-ray sources. Twenty-six of the sources in Table 1 are identified with stars known to be variable. Five of these, KM, LL, AD, KR, and V356, have been identified (18, 19) as young stellar objects. Little is known about the remaining x-ray sources in the image. They are identified in Table 1 and Fig. 1 by their Parenago designation (20). We suspect that they are optically fainter members of the nebular variable class.

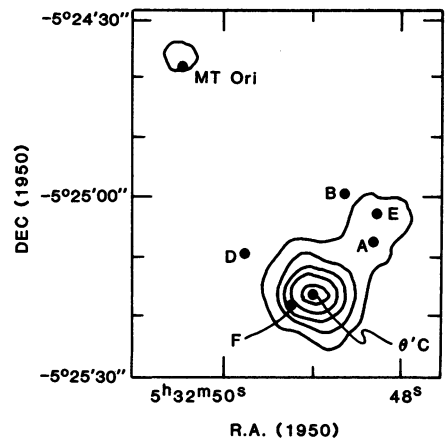
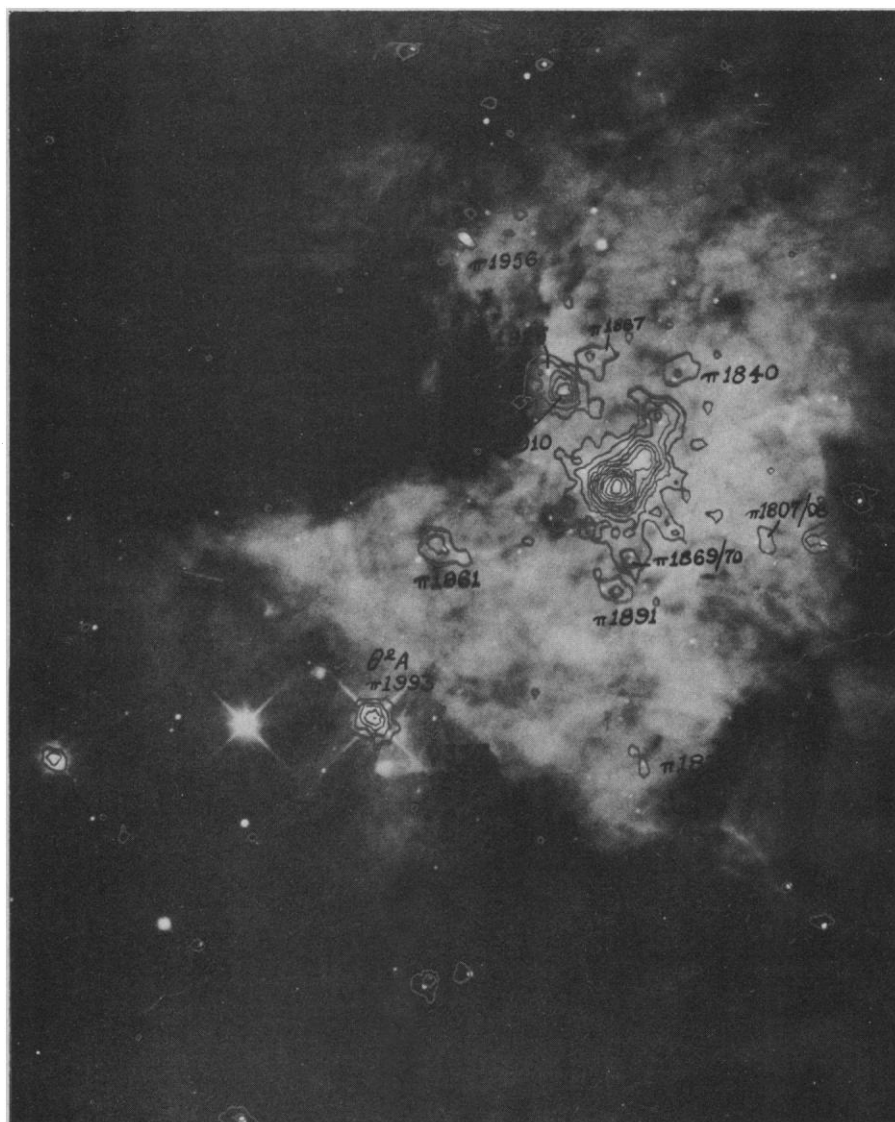


Fig. 1 (left). The central 6 arc minutes of the high-resolution x-ray image of the Orion region, superposed on a photograph of the nebula. Isophotes of x-ray emission are drawn at the levels 0.01, 0.02, 0.05, 0.07, 0.10, 0.14, 0.18, 0.23, 0.28, 0.40, 0.57, and 0.80 of the peak value of the total counts detected per square arc second. The most intense x-ray emission is from the Trapezium region, which is shown in detail in Fig. 2. The other stellar x-ray sources are designated by their usual identification or by their Parenago catalog number (20). Fig. 2 (right). X-ray emission of the Trapezium region. Dots indicate the astrometric positions of the Trapezium stars. Isophotes of x-ray emission are smoothed with a Gaussian of width 1.8 arc seconds and drawn at the levels of 2, 5, 9, 14, and 20 counts per square arc second.

X-ray emission is detected at the position of the infrared Becklin-Neugebauer (BN) object, believed to be a protostar. Due to the weakness of the emission we cannot separate BN from the two nearby stars  $\pi$ 1839 and  $\pi$ 1840. Since most of the other x-ray sources in this field are identified with stars, we consider the identification of this source with either or both of the stars as the more likely possibility. We note, however, that Pravdo and Marshall (21) recently presented evidence for x-ray emission from a protostellar object: Herbig-Haro 1 in the Orion region.

In the 25 days separating our two observations of this region, the x-ray intensities of several sources changed. The counting rate from  $\theta^1$ C increased from  $60.0 \pm 2.0$  to  $82.5 \pm 2.7$  counts per 1000 seconds from the beginning to the end of September. During one 1000-second period the flux was as high as  $121 \pm 11$  counts. Shorter term fluctuations from this bright source were also observed but with less statistical significance. Four other sources showed significant long-term changes in intensity:  $\theta^1$ E,  $\pi$ 2085, MT Ori, and AN Ori. The first two of these also showed fluctuations on a time scale of a few thousand seconds. Many other sources were observed to vary at the level of 2 to 3 standard deviations, suggesting that x-ray variability is characteristic of many of these young stars.

The spectrum and x-ray flux of  $\theta^1$ C may be estimated from IPC data because  $\theta^1$ C is at least a factor of 5 stronger than the other Trapezium sources. The best fit to the IPC data gives an optically thin thermal bremsstrahlung source temperature of  $2 \times 10^7$  K and an x-ray flux of  $2.0 \times 10^{-11}$  erg cm $^{-2}$  sec $^{-1}$ , observed through a column of material (with cosmic abundance distribution) of  $2 \times 10^{21}$  hydrogen atoms per square centimeter. At a distance of 500 pc, the x-ray luminosity of  $\theta^1$ C is  $\sim 6 \times 10^{32}$  erg sec $^{-1}$ , or about 1 million times the x-ray luminosity of the quiet sun. In the normal interstellar medium, the derived gas column density would correspond to visual extinction by dust of  $A_V \sim 1$  magnitude, in agreement with the observed visual extinction to  $\theta^1$ C (15). Because of the uncertainties in the IPC response, best-fit spectral parameters are subject to large errors. We estimate the uncertainty in the temperature and column density values to be about 50 percent and that in the flux 30 percent.

In the bremsstrahlung interpretation for  $\theta^1$ C, a volume emission measure of  $N_e^2 V \sim 1 \times 10^{56}$  cm $^{-3}$  is required to account for the observed x-ray flux from a gas at  $2 \times 10^7$  K obscured by matter of

column density  $N_H L \sim 2 \times 10^{21}$  cm $^{-2}$  ( $N_e$  is the electron density,  $V$  the volume,  $N_H$  the hydrogen number density, and  $L$  the length of the obscuring region). To avoid catastrophic self-obscuration we take  $N_H \Delta R \leq 2 \times 10^{21}$  cm $^{-2}$ , where

$\Delta R$  is the thickness of the emitting region (this allows for the possibility that the x-ray obscuration may take place either in or outside the emitting region). From the emission measure, this sets a limit of  $R(R/\Delta R) > 2 \times 10^{12}$  cm for the

Table 1. X-ray sources in the central Orion region.

Source	X-ray centroid*		X-ray flux†		Star	
	Right ascension (1950) (hr, min, sec)	Declination (1950) (deg, min, sec)	$10^{-13}$ erg cm $^{-2}$ sec $^{-1}$	Parenago No. (20)	Other designation	Spectral type (reference)
1	5 32 17.7	-5 27 00	3.9	1587		
2	23.1	25 56	1.6	1633		
3	28.7	25 06	9.4	1659	KM	K1 (19)
4	30.1	33 32	1.4	1667	KO	
5	32.5	24 56	1.7	1684	KR	K6 (19)
6	33.7	26 03	2.5	1694		
7	34.7	28 29	2.3	1704		
8	34.8	17 33	1.8	1703	V403	
9	35.8	31 57	1.5	1727	KZ	
10	38.3	27 12	3.7	1746	LL	K3 (19)
11	41.9	31 51	2.2	1773	V356	K3 (19)
12	(42.3	25 22)	6.8	1771		
13	43.1	28 12	3.2	1785	LR	
14	43.3	25 37	7.4	1784	LQ	
15	44.2	27 57	2.8	1800	LU	
16	44.9	25 36	2.3	1808/07	-/LV	
17	46.5	32 48	1.7	1827	V488	
18	46.6	21 47	1.8	1836		
19	46.6	23 13	2.2	?		
20	(47.4	24 28)	2.1	1839/40		
21	(47.8	24 44)	13.5	1862/41/42	V348/-/-	
22	48.2	27 05	2.8	1872		
23	(48.3	25 04)	36.4	1864	$\theta^1$ E	F8Vn (11)
24	(48.3	25 44)	5.5	1870/69		
25	49.0	25 16	198.0	1891	$\theta^1$ C	O7V (10)
26	(49.0	25 55)	3.6	1895		
27	49.6	23 24	2.1	1884	AE	
28	49.8	34 36	1.7	1897		
29	50.1	27 36	1.9	1914		
30	50.2	24 01	2.0	1886		
31	(50.3	24 38)	21.8	1910	MT	
32	(50.5	24 29)	2.3	1925		
33	50.7	17 31	1.6	?		
34	50.9	18 31	5.3	1906	MS	
35	51.0	24 23	3.1	1887/1909	-/AD	
36	51.2	22 26	1.6	1922	MV	
37	52.7	22 45	2.1	1937	TU	KO (20)
38	52.9	28 31	2.4	1962		
39	53.1	23 37	2.5	1956		B8IV-V (34)
40	53.5	14 07	2.5	1955		GO-2III (34)
41	53.8	25 41	6.6	1961	V494	
42	53.9	26 50	2.7	1974	V377	
43	53.9	28 37	5.1	1975		
44	54.8	22 23	2.2	1972		
45	55.5	26 50	15.9	1993	$\theta^2$ A	O9V (34)
46	55.7	20 43	1.7	1989		
47	56.6	32 38	6.6	2001	V358	G8V (35)
48	59.0	29 28	4.6	2033		
49	33 00.1	28 20	2.1	2047		
50	02.7	34 42	3.8	2069		
51	03.7	20 47	2.8	2075		
52	03.8	17 25	1.5	2073		
53	03.9	27 08	3.7	2085	$\theta^2$ C	B5V (34)
54	05.1	33 01	2.0	2100		
55	07.6	31 05	4.4	2112	V803	
56	14.6	30 03	10.7	2167	AN	K1IV (12)
57	19.9	24 39	2.0	2209		
58	24.8	30 30	2.7	2253	AQ	KO (20)

\*Due to source confusion, x-ray centroids in parentheses are nominal positions. †X-ray fluxes in the range 0.1 to 4 keV are derived by multiplying the HRI counting rate by  $2.6 \times 10^{-10}$  erg cm $^{-2}$  sec $^{-1}$ .

size and thickness of the emitting region. This requirement is consistent with the constraint of  $R < 10^{16}$  cm set by the observation that the core of the x-ray-emitting region is smaller than 1 arc second and the more severe constraint of  $< 3 \times 10^{13}$  cm set by the observation of intensity variations on the time scale of 1000 seconds.

While thermal bremsstrahlung from hot plasma is a reasonable interpretation of the x-ray data, detailed models for the x-ray emission from  $\theta^1$ C or any of the other stars in the Orion Nebula do not exist. Several scenarios for emission from early-type stars with strong stellar winds have been proposed. Our data and other Einstein data on OB stars (5, 6, 22–24) constrain some of these wind models. Cold stellar winds seem to be ruled out by the higher temperatures observed. Strong shock heating and the formation of large circumstellar bubbles (25) conflict with our observation of a small emission region for  $\theta^1$ C. Colliding winds from  $\theta^1$ C and other Trapezium stars (26) may not be ruled out (see Fig. 2), but they cannot account for more than a few percent of the total x-ray emission from  $\theta^1$ C. Hybrid models invoking hot coronas at the base of cold stellar winds (27) may eventually yield the right explanation for early-type stars. X-ray emission from late-type stars is also not well understood. In addition to coronal models (28), accretion and outflow models (29, 30) have been applied to x-ray observations with limited success. The observation of x-ray emission from a wide variety of field stars by the Einstein Observatory (31, 32) led Vaiana *et al.* (31) and others to suggest that magnetically dominated coronas, similar to that on our sun, must play an important role in all stars. Our observations of the Orion Nebula and other Einstein observations of the Pleiades and the Hyades (33) suggest that age and activity, as evidenced by rotation and magnetic fields, also play a part—that is, younger stars with active coronas produce more x-rays. Further analysis of the 29-month Einstein data base should improve our understanding of stellar dynamics and stellar evolution.

W. H.-M. KU

Columbia Astrophysics Laboratory,  
Departments of Physics and  
Astronomy, Columbia University,  
New York 10027

G. RIGHINI-COHEN  
M. SIMON

Astronomy Program, Department of  
Earth and Space Sciences,  
State University of New York,  
Stony Brook 11794

#### References and Notes

- G. Wynn-Williams, *Sci. Am.* **245** (No. 2), 46 (1981).
- R. Giacconi *et al.*, *Astrophys. J.* **230**, 540 (1979).
- R. Giacconi, S. Murray, H. Gursky, E. Kellogg, E. Schreier, T. Matilsky, D. Koch, H. Tananbaum, *ibid.* **188**, 667 (1974).
- H. V. Bradt and R. L. Kelley, *Astrophys. J. Lett.* **228**, L33 (1979).
- W. H.-M. Ku and G. A. Chanan, *ibid.* **234**, L59 (1979).
- F. R. Harnden, Jr., *et al.*, *ibid.*, p. L51.
- G. H. Rieke, F. J. Low, D. E. Kleinmann, *ibid.* **186**, L7 (1973).
- R. Cruddace, R. Paresce, S. Bowyer, M. Lampton, *Astrophys. J.* **187**, 497 (1974).
- The other sources will be described in a later publication (W. H.-M. Ku, G. Righini-Cohen, M. Simon, in preparation).
- P. S. Conti and W. R. Alschuler, *Astrophys. J.* **170**, 325 (1971).
- H. Abt, personal communication.
- M. V. Penston, *ibid.* **183**, 505 (1973).
- D. S. Hall and L. M. Garrison, Jr., *Publ. Astron. Soc. Pac.* **81**, 771 (1969).
- M. F. Walker, *Astrophys. J.* **155**, 447 (1969).
- A. B. Underhill, *The Early Type Stars* (Reidel, Dordrecht, Netherlands, 1966).
- J. S. Glasby, *The Nebular Variables* (Pergamon, New York, 1974).
- E. D. Feigelson and W. M. DeCampli, *Astrophys. J. Lett.* **243**, L89 (1981).
- G. H. Herbig, *Adv. Astron. Astrophys.* **1**, 47 (1962).
- M. Cohen and L. V. Kuhl, *Astrophys. J. Suppl.* **41**, 743 (1979).
- P. P. Parenago, *Tr. Stenberg Astron. Inst.* **25** (1954).
- S. H. Pravdo and F. E. Marshall, preprint.
- F. D. Seward, W. R. Forman, R. Giacconi, R. E. Griffiths, F. R. Harnden, Jr., C. Jones, J. P. Pye, *Astrophys. J.* **234**, L55 (1979).
- K. S. Long and R. L. White, *Astrophys. J. Lett.* **239**, L65 (1980).
- T. P. Snow, Jr., W. Cash, C. A. Grady, *ibid.* **244**, L19 (1981).
- R. Weaver, R. McCray, J. Castor, *Astrophys. J.* **218**, 377 (1977).
- B. A. Cooke, A. C. Fabian, J. E. Pringle, *Nature (London)* **273**, 645 (1978).
- J. P. Cassinelli *et al.*, preprint.
- G. S. Vaiana and R. Rosner, *Annu. Rev. Astron. Astrophys.* **16**, 393 (1978).
- R. Mundt, preprint.
- J. P. Cassinelli, *Annu. Rev. Astron. Astrophys.* **17**, 275 (1979).
- G. S. Vaiana *et al.*, *Astrophys. J.* **245**, 163 (1981).
- D. J. Helfand and J. P. Caillault, preprint.
- R. A. Stern, M. C. Zolcinski, S. K. Antiochos, J. H. Underwood, preprint.
- W. H. Warren and J. E. Hesser, *Astrophys. J. Suppl.* **34**, 115 (1977).
- G. H. Herbig and M. K. Ray, *Astrophys. J.* **174**, 401 (1972).
- We thank F. Seward for assistance at the Center for Astrophysics, H. Abt for spectral classification of  $\theta^1$ E, and F. Fallon for communicating astrometric positions of some of the Orion stars. G. Righini-Cohen and M. Simon are guest investigators with the Einstein Observatory, which is sponsored by the National Aeronautics and Space Administration and operated by a consortium of scientists from the Center for Astrophysics, Columbia University, Goddard Space Flight Center, and Massachusetts Institute of Technology. W.H.-M.K. was supported in part by NASA grant NAS 8-30753.

4 June 1981; revised 17 September 1981

## Phagocytosis: Flow Cytometric Quantitation with Fluorescent Microspheres

**Abstract.** *The phagocytosis of uniform fluorescent latex particles by pulmonary macrophages in the rat was analyzed by flow cytometric methods. The percentage of phagocytic macrophages and the number of particles per cell were determined from cell-size and fluorescence histograms. A comparison of in vivo and in vitro phagocytosis data showed that the percentage of phagocytic lavaged macrophages reflected the availability of instilled particles. With sodium azide used to model phagocytosis inhibition, it was shown that the percentage of phagocytic cells and the number of particles per cell can be determined simultaneously.*

The phagocytosis of inhaled microorganisms and inert particles by pulmonary alveolar macrophages (PAM's) is the primary cellular defense mechanism within the lung (1). Any agent that depresses or alters phagocytic action adversely affects the host's susceptibility to disease or destructive lung damage (2). Two frequently used criteria of phagocytosis are the percentage of cells having phagocytized one or more particles and the actual number of particles per cell determined microscopically (3). The procedure used to measure these values is tedious and time-consuming, and only a small sampling of the total cell population is obtained. Other methods, such as the use of radiolabeled biological material (4), are faster but provide no information on the actual proportion of cells that are phagocytic.

We have developed a phagocytosis assay in which cells are incubated with uniform fluorescent latex particles and

are analyzed by automated flow cytometric (FCM) cell-analysis methods (5, 6). This technique permits rapid quantitation of the percentage of phagocytic cells within the total population and the number of phagocytized spheres per cell. We measured in vivo phagocytosis by instilling  $1 \times 10^7$  to  $2 \times 10^7$  green fluorescent latex spheres (1.83  $\mu$ m in diameter) (7) suspended in 0.5 ml of saline into the lungs of anesthetized (15 mg of methohexital sodium, intramuscular) Sprague-Dawley rats. Two hours later the lungs were lavaged four times with 5 ml of saline containing 5 percent newborn bovine serum. Cells were layered over 3 ml of newborn bovine serum and centrifuged for 10 minutes at 360g. The cells were pelleted while the nonphagocytized spheres remained at the serum-saline interface. Cells were then washed in saline and fixed for 30 minutes in 70 percent ethanol. Before automated analysis, the cells were centrifuged to remove ethanol